JOURNAL OF SPACECRAFT AND ROCKETS
Vol. 43, No. 5, September–October 2006

Distributed and Localized Active Vibration Isolation in Membrane Structures

Hiraku Sakamoto* and K. C. Park†
University of Colorado at Boulder, Boulder, Colorado 80309-0429
and
Yasuyuki Miyazaki‡
Nihon University, Chiba 274-8501, Japan

DOI: 10.2514/1.20864

Once a membrane starts vibrating, suppressing the vibration is very difficult. Thus, the present study primarily aims at isolating a membrane from major disturbance sources, that is, from support structures. The present study introduces weblike suspension cables around a membrane and develops in theory a vibration-isolation strategy applied only along the cables. First, collocated small actuators/sensors are attached at the interfaces of the cables and the membrane to realize a distributed cable-tension control. Second, linear theory-based localized controllers are designed for suspension-cable substructural models. The feedback laws for these two kinds of controllers are derived employing a partitioned equation of motion. The resultant control system is lightweight, simple, low order, robust, and redundant. A series of transient analyses using a geometrically nonlinear finite-element method corroborates the effectiveness of the proposed vibration-isolation strategy.

Nomenclature

A	=	cross-sectional area
$\mathbf{A}$	=	state matrix
$\mathbf{B}$	=	control influence matrix
$\mathbf{B}_h$	=	actuator influence matrix for substructure controller
$\mathbf{B}_\lambda$	=	actuator influence matrix for interface force canceling controller
$\mathbf{C}$	=	constraint Boolean matrix
$\mathbf{D}$	=	partitioned damping matrix
$\mathbf{D}_g$	=	assembled damping matrix
E	=	Young's modulus
f	=	function
$\mathbf{f}$	=	partitioned nodal external force vector
$\mathbf{f}^D$	=	nodal d'Alembert's force vector
$\mathbf{f}_g$	=	global nodal external force vector
$\mathbf{f}_u$	=	control force vector
$\mathbf{G}_h$	=	feedback gain matrix
$\mathbf{G}_{h1}$	=	gain matrix for displacement
$\mathbf{G}_{h2}$	=	gain matrix for velocity
h	=	thickness
$\mathbf{I}$	=	identity matrix
J	=	scalar performance/cost index
$\mathbf{K}$	=	partitioned stiffness matrix
$\mathbf{K}_g$	=	assembled stiffness matrix
$\mathbf{K}_i$	=	stiffness matrix of ith substructure
$\mathbf{L}$	=	assembly Boolean matrix
$\mathbf{M}$	=	partitioned mass matrix
$\mathbf{M}_g$	=	assembled mass matrix
$\mathbf{P}$	=	Riccati matrix for optimal control
$\mathbf{Q}$	=	state weighting matrix
$\mathbf{q}$	=	partitioned nodal displacement vector
$\mathbf{q}_g$	=	global nodal displacement vector
$\mathbf{R}$	=	control input weighting matrix
t	=	time
$\mathbf{u}$	=	control input
$\mathbf{u}_h$	=	control input of substructure controller
$\mathbf{u}_\lambda$	=	control input of interface force canceling controller
v_0	=	amplitude of prescribed velocity
$\mathbf{x}$	=	state vector
x, y, z	=	Cartesian coordinates
α_b	=	scalar weighting of strain energy
β_b	=	scalar weighting of kinetic energy
$\Delta T_{\lambda i}$	=	tension change in ith interface force canceling controller
$\Delta \hat{T}_{\lambda i}$	=	generated tension in ith interface force canceling controller
$\Delta \varepsilon_{\lambda i}$	=	strain change in collocated sensors/actuators at ith boundary node
$\Delta \mathbf{f}_\lambda$	=	residual transmission force between substructures
Δt	=	time step size
ε	=	design strain
$\boldsymbol{\lambda}_b$	=	localized Lagrange multiplier vector
λ_{bi}	=	ith component of $\boldsymbol{\lambda}_b$
ν	=	Poisson's ratio
Π	=	total energy functional
ρ	=	density

Subscripts

h	=	homogenous localized-substructure controller
ic	=	inner-catenary cable
m	=	membrane
opc	=	outer-perimeter cable
tie	=	tie cable
λ	=	interface force canceling controller (cable-tension controller)

Received 2 November 2005; accepted for publication 26 February 2006.

*JSPS Postdoctoral Fellow, Center for Aerospace Structures, UCB 429; Hiraku.Sakamoto@Colorado.EDU. Member AIAA.

†Professor, Center for Aerospace Structures and Department of Aerospace Engineering Sciences, UCB 429. Associate Fellow AIAA.

‡Associate Professor, Department of Aerospace Engineering, College of Science and Technology, 7-24-1 Narashinodai, Funabashi, Chiba 274-8501, Japan.

I. Introduction

MEMBRANE structures are considered viable among proposed large space structures that will make innovative missions possible, such as solar sails, large reflectors, and sun shields. The ultralow areal density of membranes is attractive for achieving high packaging efficiency, which is unattainable by other conventional

structures. However, lightly prestressed membranes have very low vibration frequencies and small damping, making vibration control of the structures extremely challenging. Since *passive* damping effects in membranes are less expected than in conventional structures, membrane structures demand more intensive *active* control systems [1]. However, attaching actuators and sensors directly on membranes makes the system heavy, significantly impairing the mass advantage of "gossamer" structures. In addition, complex control systems degrade the reliability.

The present paper proposes to introduce simple controllers only along the suspension cables around a membrane. Since vibration control in a membrane itself is very difficult, the proposed controllers primarily aim at *isolating* the membrane from major disturbance sources, that is, from compressive-support structures. This study conducts a series of numerical simulations to demonstrate the effectiveness of the proposed vibration-isolation concept. The proposed control system consists of two kinds of controllers: linear theory-based localized controllers and distributed cable-tension controllers. The partitioned equation of motion provides control laws for each controller. The resultant control system is lightweight, simple, low order, robust, and redundant; thus, it is suitable for membrane space structures.

The web-cable girded membrane design, as is illustrated in Fig. 1, was proposed in the present authors' previous papers [2,3]. Employing this web-cable girded design is an essential step for the vibration-isolation strategy addressed in this paper. As we discussed in [2], the web-cable design realizes a uniformly biaxially prestressed state throughout the membrane, requiring only minimal suspension-cable mass. In [3], the authors demonstrated the effectiveness of linear theory-based substructure controllers integrated only along the weblike outer-perimeter cables. The present paper extends the concept by combining the substructure controllers with distributed cable-tension controllers. As we observed in the previous study, in the proposed design, the disturbance that emanates from the support points first triggers the motion of the web cables around the membrane. Thus, it is reasonable to apply force transmission attenuators at the cable/membrane interfaces to mitigate the vibration propagation from the web cables into the membrane. The proposed design facilitates the introduction of many small actuators along the web cables to control the cable tension. The present study shows that these distributed cable-tension controllers have larger impact on the membrane-vibration isolation than the web-cable substructure controllers. Furthermore, unlike the linear theory-based controllers, the cable-tension controllers are always stable even when the structure is subject to a large deformation.

Emerging membrane materials are making feasible the practical design of membrane structures. To balance the membrane with equally lightweight and flexible control systems, we also need to use emerging actuation and sensing devices, such as piezoelectric actuators and noncontacting sensors. The vibration-isolation strategy proposed in this paper reasonably assumes the use of such new technologies. Section II reviews these technologies and explains how they are employed in the present study. Section III proposes a concept of the localized vibration-isolation strategy for membrane structures, and Sec. IV derives the control laws. Section V evaluates the proposed strategy by carrying out a series of transient analyses using a geometrically nonlinear finite-element (FE) method allowing for membrane wrinkling. Section VI uses an FE model with compressive booms to extend the proposed vibration-isolation strategy to an overall structural system. Finally, Sec. VIII concludes the paper.

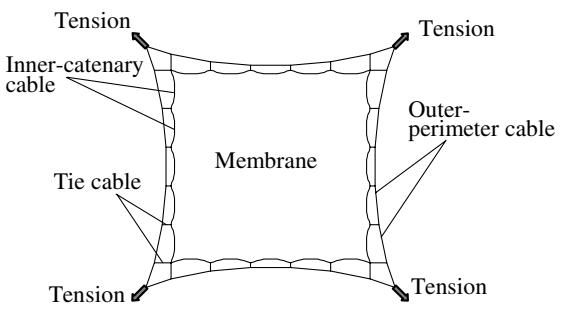

Fig. 1 Proposed web-cable girded membrane design [2,3].

II. Technological Development for Adaptive Gossamer Structure Design

A. Advanced Materials and Actuation/Sensing Technologies

The present study assumes the use of the following materials and devices. CP1 [4,5] is used for casting a membrane. Piezoelectric actuators, such as macrofiber composite (MFC) actuators [5,6], are used for distributed cable-tension controllers. In addition, noncontact sensing by videogrammetry [7,8] is assumed for linear theory-based substructure controllers; however, both measurement errors induced by the sensing device and state-estimation errors in controllers are ignored in the analyses for simplicity. In future studies, these assumptions should be relaxed and the effect of these errors should be investigated for more practical applications.

B. Techniques for Modeling Membrane Dynamics

Recent developments in mechanics have enabled geometrically nonlinear analyses, which significantly advance the practical design of adaptive gossamer structures. For membrane modeling, geometrical nonlinearity has to be properly taken into account, because the stiffness of the membranes heavily depends upon their loading conditions. Recent research efforts in membrane modeling are summarized in [9]. The present study adopts the same geometrically nonlinear FE method as the previous studies, which was developed by Miyazaki [9]. Membranes are modeled by 4-noded quadrilateral planar-stress elements, whose constitutive matrix is modified by a tension-field (TF) theory-based scheme to account for wrinkling. Dynamic analysis is carried out by an energy momentum-conserving method [10]. The numerical-simulation results show a good correlation with experimental results [11]. All codes are handwritten on MATLAB.

Numerical modeling errors of the adopted method from the analytical solutions are investigated using simple models. A square-membrane FE model and a cantilever-beam FE model are examined. First, a 12×12 meshed square-membrane model with all sides fixed predicts the first 15 mode frequencies within 4.4% errors from the analytical solutions. Second, a cantilever-beam model is constructed with 10 Timoshenko beam elements, which are used in Sec. VI. This FE model predicts the first three mode frequencies of the beam within 3.8% errors from the analytical solutions. The presence of an axial force does not degrade the mode-frequency prediction. (The analytical solutions for the vibrational frequencies of the beam under axial force are obtained by Shaker [12].) Accordingly, the present authors conclude that the numerical method employed in this study has sufficient accuracy to observe the fundamental vibrational characteristics of membrane structures.

III. Concept of Localized Control Strategy

A. Introduction

1. *Control Objective*

The design objective pursued in this study is to suppress vibration in a membrane over the course of space missions. Such suppression is extremely challenging for the following three reasons.

1) A lightly prestressed membrane has very low mode frequencies, especially in the out-of-plane direction; thus, it is prone to vibration even for small disturbance loads.

2) Because membrane deformation creates only minimal strain change in materials, the effect of passive damping is small.

3) Putting many actuators and sensors, or passive dampers, directly on a membrane significantly impairs the mass and flexibility advantage of membrane structures.

Accordingly, the present study explores introducing intensive active controllers only along suspension cables around a membrane. These controllers aim primarily at isolating the membrane from

major dynamic disturbance sources, that is, from compressive-support structures. Because other disturbance loads imposed directly on a membrane in space are quasistatic, the proposed strategy will alleviate membrane vibration over the course of a mission. The detailed strategy is presented in Sec. III.C.

This paper considers membrane vibrations only in the out-of-plane direction, because the membrane's in-plane mode frequencies are much higher than those in the out-of-plane direction [3]. However, when the in-plane vibration is coupled with the out-of-plane vibration, its effect is yet unknown. In future studies, this coupling effect must be investigated.

2. *Requirements for Control System in Membrane Structures*

The control methods for membrane structures have to satisfy the following five requirements.

R1) Lightweight: Because small mass is one of the most important properties in gossamer structures, the control system also needs to be lightweight. This means that only a minimum number of small actuators and sensors can be used; in addition, the mass and volume of processors should be minimized.

R2) Simplicity: Gossamer structural elements are very thin and flexible; thus, wiring controllers together would be difficult. As a result, the controllers should be as distributed and autonomous as possible.

R3) Low order: Because the on-board processors need to be small, as discussed in item R1, the controller should be as low order as possible to minimize the computational effort.

R4) Robustness to uncertainty: The operational conditions that spacecraft in orbit confront are very uncertain. For example, unpredicted accidents can vary the thermal, radiational, or gravitational conditions. In addition, because membrane structures have a strong geometrical nonlinearity, the structural response itself is also less predictable. Thus, the control system has to be robust enough so that stability is ensured even when the system is largely perturbed from the original model.

R5) Redundancy for local failures: Because the gossamer structural elements are usually fragile, we expect some local failures during the course of operation. Therefore, the control system should be redundant, so that the function of the overall system is preserved even when structural and/or control systems have local failures.

To satisfy the requirements listed above, the present authors propose a *localized control strategy*, one especially suitable to attenuate vibration in membrane structures.

B. Preceding Studies

1. *Studies on Shape and Vibration Control in Gossamer Structures*

For the last decade, shape controls of membrane surfaces have been discussed with a rim actuation [13–15] or a membrane interior actuation [16–23]. However, only a few studies have been devoted to membrane-vibration mitigation. Natori [24] proposed a nonlinear vibration control for a membrane that changes support tensions at the membrane edges. Although this is theoretically attractive, its practical realization will be difficult. Sodano et al. [25] carried out a vibration-control experiment of an inflatable torus using MFC actuators. They successfully controlled the first mode vibration of the torus and also proposed a self-sensing controller using collocated sensors/actuators. Solter et al. [26] also carried out an experiment using an inflatable torus with a flat membrane reflector. Two kinds of piezoelectric actuators are located at the same connecting points between the torus and the membrane: a piezoelectric stack changes tension in a support cable, and an MFC bimorph provides an out-of-plane actuation. A single-input single-output (SISO) feedback decayed the frequency-response amplitude around a target frequency. Glaese and Bales [27] added masses and mass dampers to a similar inflatable-torus structure to improve its vibrational characteristics. In addition, collocated piezoelectric sensors/actuators are attached at torus/membrane interfaces to demonstrate several control laws, including a six-input six-output linear quadratic (LQ) control.

The present study considers a membrane structure suspended with a large span. In this type of membrane structure, one has to take into account the geometrical nonlinearity. This study proposes a control method allowing for the geometrical nonlinearity of a membrane. The significance of the proposed strategy is that it combines the multi-input multioutput (MIMO) substructure-based LQ controllers and the distributed cable-tension controllers. This is achieved by invoking the *localized control theory* by Park and Kim [28].

2. *Studies on Localized Control Concept*

The problem of controlling flexible structures, such as large space structures, is often called the control/structure interaction (CSI) problem. The CSI problem has been an active area of research during the past decade. Some researchers working on the CSI problem proposed the distributed (or decentralized) control approach to substantially reduce the controller order and the system complexity. Young [29], Sunar and Rao [30], and Su et al. [31] proposed substructure-based localized controllers. They used LQ optimal controllers, although any other controller can be used, for the substructure control, and combined it with the controllers that attenuate the coupling effects between the substructures. A similar approach can be found in older literatures, such as Balas and Canavin [32]. They proposed a control law to be composed of two parts:

$$\mathbf{u} = \mathbf{u}_c + \mathbf{u}_d \tag{1}$$

The part $\mathbf{u}_c$ is provided by a LQ-substructure controller, which attempts to stabilize the substructure. The part $\mathbf{u}_d$ attempts to counteract disturbances emanated from other adjoined substructures.

Cable-suspended membrane structures that are considered in the present study have the following particular nature. In the suspension cables, the tension can be directly measured by strain gages. In addition, the cable tension can be controlled by attaching small actuators, such as piezoelectric actuators. This fact implies that the internal-transmission force in the suspension-cable substructures can be exploited both for state estimation and for controller input. This observation motivates us to use the localized control theory by Park and Kim [28] in the proposed web-cable girded design. The Park–Kim controller uses the Lagrange multipliers, essentially internal-transmission forces. Morita and Park [33] discussed the robustness enhancement of the Park–Kim localized controller by introducing an H_∞ optimal estimator, and numerical simulations demonstrated the effectiveness of the localized control strategy. The present study modifies the original concept of Park and Kim to one suitable for the cable-suspended membrane structures.

The redundancy in gossamer structures, described in item R5, has been addressed by some researchers. Ishimura et al. discussed a redundancy concept in large space structures and applied autonomous-distributed controllers to a variable-geometry truss manipulation [34] and a two-dimensional panel deployment control [35]. Their analyses suggest that the autonomous-distributed controllers in large space structures still maintain their global function even when there are some local failures in structural or control systems. Sakamoto et al. [36] proposed redundant inflatable structures with multicellular membrane envelopes. By making them multicellular, the effect of envelope punctures due to space debris or meteoroid collisions can be limited in local regions; as a result, the global structure maintains its function. As is seen previously, introducing redundancy in gossamer structures is an effective method both for structural and control systems. It protects a vulnerable system from global disfunctioning without resorting to a significant increase in mass.

C. Concept of Proposed Localized Control Strategy

In [3], we observed that the membrane in the conventional catenary design [37] is easily subject to vibration when perturbations occur at the support corners. By contrast, in the proposed web-cable girded design, the vibration that emanates from the support points first triggers motions of the web cables. Thus, it is reasonable for us to put controllers on these cables to dissipate the vibration energy

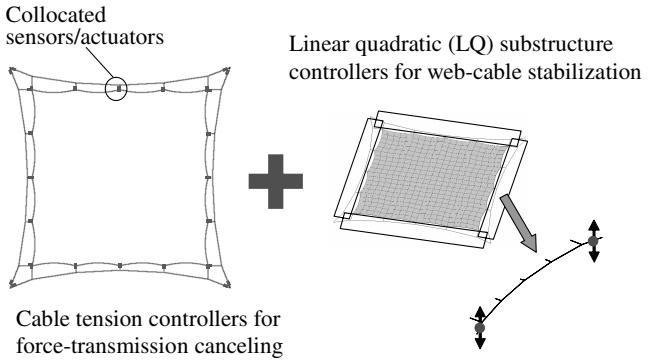

Fig. 2 Concept of proposed dual-control system.

before it propagates into the membrane. Accordingly, the present study proposes a two-step membrane vibration-isolation strategy, as Fig. 2 illustrates. First, small actuators are attached at the interfaces between the web cables and the membrane. These actuators modify the cable tension. Second, LQ regulators are applied to the web-cable substructures. The actuators are attached only near the support corners, and they provide control forces in the out-of-plane direction. The proposed strategy satisfies the five requirements for the control system in membrane structures, R1–R5, as follows.

First, the proposed strategy will not require any massive devices, so the control system is lightweight (R1). Second, since both LQ-substructure controllers and cable-tension controllers are completely localized and distributed, the system does not require complex wiring, enabling a simple realization (R2). Third, the LQ controllers are designed with the partitioned substructures; therefore, the controller order is substantially reduced when compared to full-model based controllers (R3). Fourth, the cable-tension controllers at the membrane/cable interfaces can employ a control law that is always stable, such as a direct velocity feedback (DVF) [38]. In addition, these cable-tension controllers work to keep the system close to the original plane; thus, the linear-model based substructure controllers can perform better with the cable-tension controllers, which mitigate the model perturbations (R4). Finally, the proposed control system is localized and distributed, so that a local failure does not result in a critical failure of the global system (R5). Hence, the proposed vibration-isolation strategy is suitable for membrane structures.

IV. Theory of Proposed Localized Controller

A. Overview

This section formulates control laws for the proposed vibration-isolation strategy. The formulas are derived based on the localized control theory by Park and Kim [28]. First, the partitioned equation of motion is formulated. Second, both a linear theory-based substructure controller and a cable-tension controller are designed. Finally, the effect of the proposed controllers in a global equation of motion is observed.

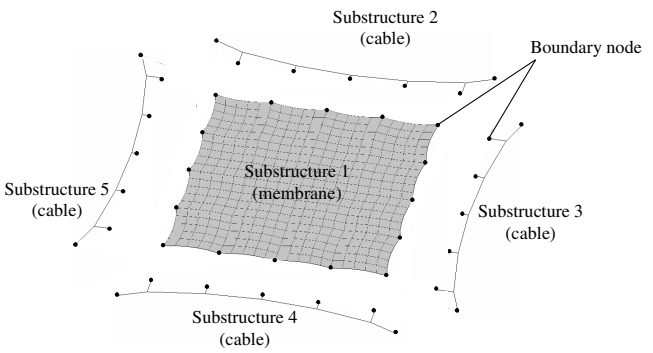

Fig. 3 Partitioned web-cable girded design.

B. Formulation of Partitioned Substructural Dynamic Equations

Using a finite-element method, the system dynamics can be approximated by the following linear matrix equation [3]:

$$\mathbf{M}_g\ddot{\mathbf{q}}_g + \mathbf{D}_g\dot{\mathbf{q}}_g + \mathbf{K}_g\mathbf{q}_g = \mathbf{f}_g \tag{2}$$

In the present study, these matrices are obtained by a geometrically nonlinear finite-element method developed by Miyazaki [9]. In the code, membranes are modeled by TF theory-based membrane elements; thus, the tangent stiffness matrix $\mathbf{K}_g$ can contain a wrinkling effect. The global system is now partitioned into substructures, as Fig. 3 illustrates, providing

$$\mathbf{K}_g = \mathbf{L}^T\mathbf{K}\mathbf{L}, \qquad \mathbf{M}_g = \mathbf{L}^T\mathbf{M}\mathbf{L}, \qquad \mathbf{D}_g = \mathbf{L}^T\mathbf{D}\mathbf{L} \tag{3}$$

where

$$\mathbf{K} = \begin{bmatrix} \mathbf{K}_1 & & & \\ & \mathbf{K}_2 & & \\ & & \ddots & \\ & & & \mathbf{K}_N \end{bmatrix}$$

The assembly Boolean matrix $\mathbf{L}$ also gives the following relations:

$$\mathbf{q} = \mathbf{L}\mathbf{q}_g, \qquad \mathbf{f} = \mathbf{L}\mathbf{f}_g \tag{4}$$

Hence, the discrete energy functional can be expressed in terms of the partitioned nodal displacements as

$$\Pi(\mathbf{q}_g, \boldsymbol{\lambda}_b, \mathbf{q}) = \mathbf{q}_g^T(\tfrac{1}{2}\mathbf{L}^T\mathbf{K}\mathbf{L}\mathbf{q}_g - \mathbf{L}^T\mathbf{f}^D) \tag{5}$$

$$= \mathbf{q}^T(\tfrac{1}{2}\mathbf{K}\mathbf{q} - \mathbf{f}^D) + \boldsymbol{\lambda}_b^T\mathbf{C}^T(\mathbf{q} - \mathbf{L}\mathbf{q}_g) \tag{6}$$

where

$$\mathbf{f}^D = \mathbf{f} - \mathbf{M}\ddot{\mathbf{q}} - \mathbf{D}\dot{\mathbf{q}} \tag{7}$$

where $\boldsymbol{\lambda}_b$ are the so-called *localized* Lagrange multipliers [39,40], which enforce the interelement kinematical compatibility condition [the first equation in Eq. (4)]. A constraint Boolean matrix $\mathbf{C}$ extracts only the partition boundary displacements. Note that the localized version of Lagrange multipliers in the above equations exactly represents physical forces applied at an interface node even when the interface node involves more than two substructural boundary nodes.

The stationary condition of the above functional, $\delta\Pi(\mathbf{q}_g, \lambda_b, \mathbf{q}) = 0$, leads to the following partitioned equation of motion:

$$\begin{bmatrix} \left(\mathbf{M}\dfrac{d^2}{dt^2} + \mathbf{D}\dfrac{d}{dt} + \mathbf{K}\right) & \mathbf{C} & \mathbf{0} \\ \mathbf{C}^T & \mathbf{0} & -\mathbf{L}_b \\ \mathbf{0} & -\mathbf{L}_b^T & \mathbf{0} \end{bmatrix} \begin{bmatrix} \mathbf{q} \\ \boldsymbol{\lambda}_b \\ \mathbf{q}_g \end{bmatrix} = \begin{bmatrix} \mathbf{f} \\ \mathbf{0} \\ \mathbf{0} \end{bmatrix} \tag{8}$$

where $\mathbf{L}_b = \mathbf{C}^T\mathbf{L}$. The first row of Eq. (8) constitutes the equilibrium equation of each substructure, and the second row corresponds to the displacement compatibility between the partition boundaries. The third row is the Newton's third law at the interfaces.

C. Construction of Localized Controller

Introducing a controller to the governing equation of motion (8), we obtain the resulting controlled substructure to be

$$\mathbf{M}\ddot{\mathbf{q}} + \mathbf{D}\dot{\mathbf{q}} + \mathbf{K}\mathbf{q} + \mathbf{C}\boldsymbol{\lambda}_\mathbf{b} = \mathbf{f} + \mathbf{f}_u \tag{9}$$

where $\mathbf{f}_u$ is the control force vector to be formulated. The control problem is thus to attenuate the response $\mathbf{q}(t)$. A key concept of the present control scheme is to construct the controller in terms of two components, similarly to Eq. (1):

$$\mathbf{f}_u = \mathbf{B}_h\mathbf{u}_h + \mathbf{B}_\lambda\mathbf{u}_\lambda \tag{10}$$

First, the homogeneous localized controller in Eq. (10), $\mathbf{u}_h$, is obtained by a LQ regulator for the undamped homogenous system:

$$\mathbf{M}\ddot{\mathbf{q}} + \mathbf{K}\mathbf{q} = \mathbf{B}_h\mathbf{u}_h \tag{11}$$

Rewriting Eq. (11) into the state space description yields

$$\dot{\mathbf{x}} = \mathbf{A}\mathbf{x} + \mathbf{B}\mathbf{u}_h \tag{12}$$

where

$$\mathbf{A} = \begin{bmatrix} \mathbf{0} & \mathbf{I} \\ -\mathbf{M}^{-1}\mathbf{K} & \mathbf{0} \end{bmatrix}, \qquad \mathbf{B} = \begin{bmatrix} \mathbf{0} \\ \mathbf{M}^{-1}\mathbf{B}_h \end{bmatrix}, \qquad \mathbf{x} = \begin{bmatrix} \mathbf{q} \\ \dot{\mathbf{q}} \end{bmatrix}$$

The following cost functional is set up:

$$J = \int_0^t \frac{1}{2}(\mathbf{x}^T\mathbf{Q}\mathbf{x} + \mathbf{u}_h^T\mathbf{R}\mathbf{u}_h)\mathrm{d}\tau \tag{13}$$

where the weighting matrices, $\mathbf{Q}$ and $\mathbf{R}$, are chosen according to Belvin and Park [41] as

$$\mathbf{Q} = \begin{bmatrix} \alpha_b\mathbf{K} & \mathbf{0} \\ \mathbf{0} & \beta_b\mathbf{M} \end{bmatrix}, \qquad \mathbf{R} = \mathbf{B}_h^T\mathbf{K}^{-1}\mathbf{B}_h \tag{14}$$

with α_b and β_b being tuning parameters. With this choice, the minimization of the cost functional in Eq. (13) corresponds to the minimization of the internal energy in the system and control effort simultaneously. Then the optimal feedback gain is given by

$$\mathbf{u}_h = -\mathbf{G}_{h1}\mathbf{q} - \mathbf{G}_{h2}\dot{\mathbf{q}} \tag{15}$$

where $\mathbf{G}_h = [\mathbf{G}_{h1}\mathbf{G}_{h2}] = \mathbf{R}^{-1}\mathbf{B}^T\mathbf{P}$, and $\mathbf{P}$ is the solution to the steady-state matrix Riccati equation. In this study, the LQ controllers are designed only for the web-cable substructures, and the membrane substructure is left uncontrolled. We also assume for simplicity that each LQ-substructure controller precisely knows the full state, $\mathbf{x}(t)$, of the corresponding web-cable substructure.

Second, the controller $\mathbf{u}_\lambda$ in Eq. (10) aims at attenuating the response due to the internal force $\mathbf{C}\boldsymbol{\lambda}_b$ acting on each partitioned substructure. The interface transmission forces can be nullified if

$$\mathbf{B}_\lambda\mathbf{u}_\lambda = \mathbf{C}\boldsymbol{\lambda}_b \tag{16}$$

In the present study, small collocated sensors/actuators, such as piezoelectric patches, are attached to the interface nodes, as Fig. 4 illustrates; therefore, the internal force $\boldsymbol{\lambda}_b$ can be directly measured by the strain sensors. The internal force at the ith partition boundary node λ_{bi} can be related to the tension change in the collocated sensors/actuators $\Delta T_{\lambda i}$ using a certain function f as

$$\lambda_{bi} = f(\Delta T_{\lambda i}) \tag{17}$$

For example, if the sensor measures and generates in-plane forces, the relationship between the out-of-plane force λ_{bi} and the in-plane force $\Delta T_{\lambda i}$ is usually nonlinear. If bimorph piezoelectric patches [26] are used, the out-of-plane internal force bends the patch, causing a tension change in the bimorph. Now assume the following constitutive relation in the small sensor/actuator:

$$\Delta T_{\lambda i} = (E_\lambda A_\lambda)_i \Delta\varepsilon_{\lambda i} \tag{18}$$

Then using the measured strain $\Delta\varepsilon_{\lambda i}$, consider the following feedback to generate the tension change $\Delta\hat{T}_{\lambda i}$ in each actuator:

$$\Delta\hat{T}_{\lambda i} = (E_\lambda A_\lambda)_i \Delta\varepsilon_{\lambda i} \tag{19}$$

As can be easily seen, this autonomous-distributed control law realizes the ideal controller in Eq. (16). In the numerical demonstration in the following sections, $\Delta\varepsilon_{\lambda i}$ is measured as a strain change between a previous time step and the current time step, as the simplest realization. This results in the control law corresponding to a DVF, which is always stable [38].

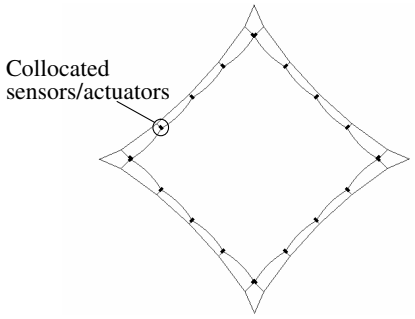

Fig. 4 Collocated sensors/actuators at cable/membrane interfaces.

D. Closed-Loop System Dynamics

By substituting Eqs. (10–16) into Eq. (9), the closed-loop system dynamic equation yields

$$\mathbf{M}\ddot{\mathbf{q}} + (\mathbf{D} + \mathbf{B}_h\mathbf{G}_{h2})\dot{\mathbf{q}} + (\mathbf{K} + \mathbf{B}_h\mathbf{G}_{h1})\mathbf{q} = \mathbf{f} + \Delta\mathbf{f}_\lambda \tag{20}$$

where $\Delta\mathbf{f}_\lambda = \mathbf{B}_\lambda\mathbf{u}_\lambda - \mathbf{C}\boldsymbol{\lambda}_b$. As can be seen in Eq. (20), the LQ controller increases both stiffness and damping of the system; in addition, the distributed controllers at the partition boundaries cancel the force transmission between the substructures, that is, $\|\Delta\mathbf{f}_\lambda\| \to 0$ as $t \to \infty$. From Bellman's theorem [42] (Theorem 3 in Chapter 13), the present closed-loop system is stable except for the rigid body dynamics, if $\mathbf{M} \geq 0$ and $(\mathbf{D} + \mathbf{B}_h\mathbf{G}_{h2})$, $(\mathbf{K} + \mathbf{B}_h\mathbf{G}_{h1}) > 0$, or $(\mathbf{K} + \mathbf{B}_h\mathbf{G}_{h1}) \geq 0$ and $\mathbf{M}$, $(\mathbf{D} + \mathbf{B}_h\mathbf{G}_{h2}) > 0$.

V. Nonlinear Transient Analysis with Proposed Control Strategy

A. Overview

The effectiveness of the proposed vibration-isolation strategy is demonstrated by a series of numerical simulations. The proposed control strategy is applied to FE models of the web-cable girded membrane design. Nonlinear transient analyses are carried out with an impulse input applied at one of the support corners. First, the effect of only the distributed cable-tension controllers is demonstrated. Second, both the LQ-substructure controller and the distributed cable-tension controller are introduced into the FE model. Furthermore, Sec. VI extends the proposed concept to a model that includes compressive-support booms.

B. Effect of Distributed Cable-Tension Controller

Figure 5 depicts the FE model with piezoelectric elements at the membrane/cable interfaces. The membrane is divided into 12×12 4-node quadrilateral TF theory-based membrane elements. The

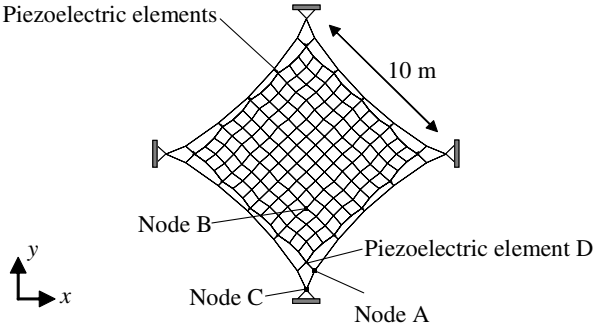

Fig. 5 Finite-element model with piezoelectric elements at membrane/cable interfaces.

Table 1 Material and design parameters in the analysis

Category	Value
Membrane (CP1):	Young's modulus, $E_m = 3.454$ GPa
	Thickness, $h_m = 5$ μm
	Poisson's ratio, $\nu_m = 0.312$
	Density, $\rho_m = 1.44$ g/cc
Cables (Hexcel® carbon fiber IM9):	Young's modulus, $E_{\text{ic}} = E_{\text{opc}} = E_{\text{tie}} = 193$ GPa
	Density, $\rho_{\text{ic}} = \rho_{\text{opc}} = \rho_{\text{tie}} = 1.79$ g/cc
Design Strain:	Membrane and inner-catenary cable, $\varepsilon_m = \varepsilon_{\text{ic}} = 14\mu$-strain
	Outer-perimeter cable and tie cable, $\varepsilon_{\text{opc}} = \varepsilon_{\text{tie}} = 0.1\%$

Table 2 Properties of piezoelectric element

Category	Value
Bulk modulus:	0.15 MPa (actuators along tie cables)
	28.4 MPa (actuators at corners, Sec. VI)
Cross-sectional area:	1.45×10^{-6} m^2
Density:	4.75 g/cc
Length:	50 mm (actuators along tie cables)
	100 mm (actuators at corners, Sec. VI)

Table 3 Fundamental mode frequencies of substructures

Substructure	Fundamental mode frequencies
Membrane + inner-catenary cable	0.51 Hz
Outer-perimeter cable + tie cable	21.7 Hz
Beam (see Sec. VI)	1.86 Hz

material and design parameters are shown in Table 1.[§] The membrane size is chosen as 10 m × 10 m. The uniform strain in the CP1 membrane, chosen at 14 μ-strain, corresponds to a uniform stress of 70.3 kPa (≈10.2 psi). The cross-sectional area of each IM9 cable is optimized so that the strain in the cable is equal to the design strain, ε_{ic}, ε_{opc}, and ε_{tie}. The piezoelectric element is basically a bar element, but its internal force can be given as a function of the element strain in the previous and current time step. The feedback law in Eq. (19) is used. The properties of the piezoelectric elements are shown in Table 2. The elasticity modulus of the piezoelectric elements is set much smaller than existing piezoelectric actuators, such as the MFC actuators [6] to magnify their effect. This small bulk modulus will be achieved, for example, by employing a piezoelectric stack or a bimorph mechanism [26]. As Fig. 5 illustrates, these piezoelectric elements are integrated into the web-cable design FE model. Twenty 50-mm long elements are located at all the interfaces between the tie cables and the membrane.

An eigenvalue analysis using this FE model, with its four corners fixed, finds the fundamental mode frequency to be 0.43 Hz. However, partitioned-structural models, as Fig. 3 shows, find that the web-cable substructures have higher mode frequencies than those of the membrane. When only the substructural nodal components are extracted from $\mathbf{K}_g$ and $\mathbf{M}_g$, the fundamental mode frequencies of each partitioned system are found as Table 3 shows. This frequency difference has a significant impact on the membrane-vibration isolation, as we discuss later.

Figures 6 and 7 show the uncontrolled and controlled displacement histories on nodes A and B in the out-of-plane direction, respectively. A velocity impulse $v_0 = 50$ m/s is applied at node C at $t = 0$. The velocity impulse in this study is generated as a 250-Hz half-period sinusoid. The time-step size is chosen as $\Delta t = 5 \times 10^{-4}$ s. As can be seen in the figures, with the cable-tension controllers, the vibration amplitude on the membrane (node B) is reduced, especially before $t = 10$ s, when compared to that of the uncontrolled response, whereas the vibration amplitude on the outer-perimeter cables (node A) is only slightly suppressed in the controlled response. This clearly shows that the cable-tension controllers attenuate the vibration propagation from the web cables to the membrane. However, the membrane-controlled response (Fig. 7b) suffers a large vibration amplitude around $t = 11$ s. This delayed vibration is mitigated by introducing the LQ-substructure controllers in the next subsection.

Figure 8 displays the force generated by the piezoelectric element D. As is seen, relatively large forces are generated when the outer-perimeter cables vibrate severely. However, as the vibration gets moderate, the generated force also decreases, because the piezoelectric element experiences less strain changes. Thus, the cable-tension controllers mainly work only when the structure is largely perturbed from the original plane. When the vibration amplitude is small, the cable-tension controllers may contribute less, whereas the LQ-substructure controllers in the next subsection work more effectively when the structure stays close to the original plane. This shows an effective collaboration of these two kinds of controllers.

C. LQ-Substructure Controllers for Web Cables

As Fig. 9 shows, the four web-cable substructures are partitioned from the global structure, and the LQ controllers are designed for each web-cable substructure. Two out-of-plane actuators are located near the support corners in each substructure. The eight actuators in total are installed into the global FE model, as Fig. 10 shows. These actuators will be attached to support structures, as is illustrated in the box in the figure. The Belvin–Park gains in Eq. (14) are set at

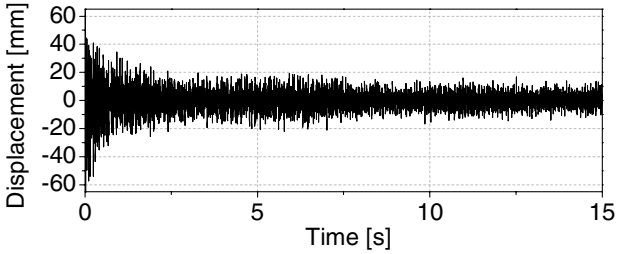

a) On outer perimeter cable (Node A)

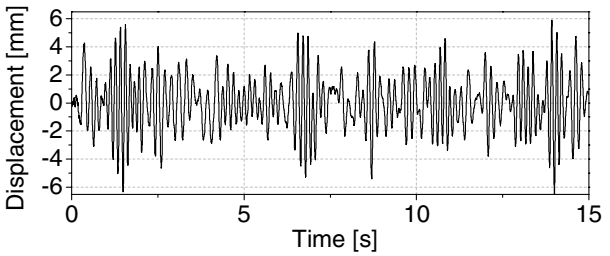

b) On membrane (Node B)

Fig. 6 Uncontrolled response: A velocity impulse is applied at node C at $t = 0$.

[§]CP1 properties are provided by courtesy of Jim Moore at SRS Technologies, Inc.

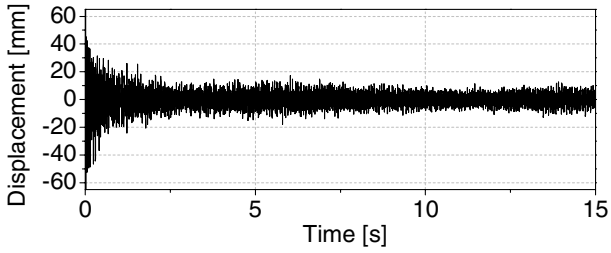

a) On outer perimeter cable (Node A)

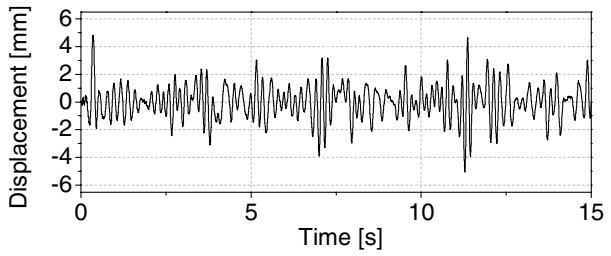

b) On membrane (Node B)

Fig. 7 Response with distributed control using piezoelectric actuators: A velocity impulse is applied at node C at $t = 0$.

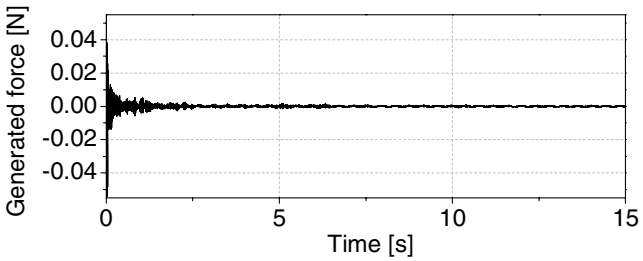

Fig. 8 Generated force in piezoelectric element D.

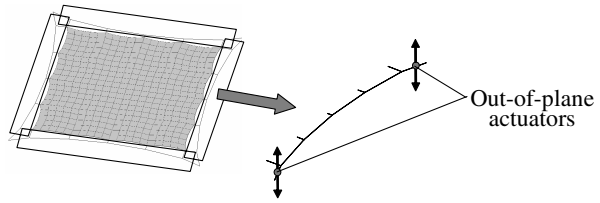

Fig. 9 Localized controller for web-cable substructures.

$\alpha_b = \beta_b = 8 \times 10^{-3}$. The same velocity impulse with the preceding analysis, $v_0 = 50$ m/s, is applied in the out-of-plane direction at $t = 0$ at node C.

Figures 11a and 11b show controlled response on the outer-perimeter cable (node A) and on the membrane (node B), respectively. In this analysis, the cable-tension controllers are also turned on. Figure 12 shows the generated forces by the piezoelectric element D and by the out-of-plane actuator at node E, respectively. As we see in Fig. 11a, the LQ-substructure controllers suppress the vibration in the web cables significantly, whereas they have only a small impact on the membrane-vibration amplitude when we compare Figs. 7b and 11b. The reason why the LQ-substructure controllers have only a small impact on membrane vibration is explained as follows. As Table 3 describes, the web-cable substructures have much higher mode frequencies than those of the membrane. Therefore, low-frequency vibration energy instantly flows into the membrane and barely excites the web-cable vibration. As a result, the web-cable substructure controllers cannot effectively counteract the low-frequency components of the disturbance. However, Fig. 11 also demonstrates a significant effect of the LQ-substructure controllers for the membrane-vibration mitigation. Unlike Fig. 7b, Fig. 11b does not show a large vibration amplitude around $t = 11$ s. This is because the LQ-substructure controllers quickly dissipate vibration in the web cables as shown in Fig. 11a; thus, the web cables stop exciting the membrane vibration after the first brunt. Consequently, the collaboration of the two kinds of controllers limits the membrane-vibration amplitude within 3 mm, which is approximately half the amplitude of the uncontrolled response in Fig. 6b.

VI. Extension of Proposed Concept to Compressive Supports

A. Addition of Compressive Supports

This section extends the proposed localized vibration-isolation concept to compressive-support structures. The support booms, as Fig. 13 illustrates, are added to the FE model used in the preceding analyses. The support booms are partitioned into four substructures, and LQ-substructure controllers are designed for these beam substructures. In addition, the cable-tension controllers are added at the beam/web-cable interfaces, that is, at the support corners of the web cables.

B. LQ-Substructure Controller for Beam

The FE model of the diagonal booms is partitioned into four substructures. Figure 14 illustrates one of the beam substructures. The compressive boom is modeled by 10 Timoshenko beam elements. The beam properties are shown in Table 4. The beam length corresponds to half of the diagonal length of the membrane structure. The axial force, 17.0 N, is equal to the cable tension of the web-cable design at the corner. Two out-of-plane actuators are located in each beam substructure. The actuator locations are shown in Fig. 14. The fundamental mode frequency of this beam substructure lies between the membrane frequency and the web-cable frequency, as Table 3 displays.

LQ controllers are designed also using the Belvin–Park method for these beam substructures. This time, the modal reduction is carried out by truncating the unmodeled modes. The first 30 modes are retained. The gains are chosen as $\alpha_b = \beta_b = 1 \times 10^{-2}$. Figure 15 shows the uncontrolled and controlled response of the cantilever-beam FE model at the tip in the out-of-plane direction. The velocity impulse $v_0 = 5$ m/s is applied at the tip in the out-of-plane direction at $t = 0$. As can be seen, the LQ controller effectively supplies the damping.

C. Beam/Membrane/Cable-Coupled Analysis

Figure 16 shows the global FE model. Four of the beam substructures are connected to the web-cable corners at the beam tips. All 6 degrees of freedom at the beam-crossing center are fixed. Note that the membrane elements are completely separated from the beam elements. No contact is considered. With these boundary conditions, the fundamental mode frequency of the global model obtained by an eigenvalue analysis is 0.23 Hz.

The four web-cable LQ-substructure controllers and the four beam LQ-substructure controllers are installed into the FE model. The piezoelectric elements are attached at all the membrane/tie-cable interfaces; in addition, two piezoelectric elements are put at each outer-perimeter-cable corner (eight in total), whose properties are shown in Table 2. In this analysis, penalty parameters for the membrane-wrinkling effect are set at $\epsilon_1, \epsilon_2 = 1$ to stabilize the computation [the definition of (ϵ_1, ϵ_2) is found in [9]]. In other words, the wrinkling effect in the membrane is not taken into account in this analysis. The velocity impulse $v_0 = 5$ m/s is applied at node C in the out-of-plane direction at $t = 0$.

Figures 17 and 18 display the uncontrolled and controlled displacements, respectively. As Figs. 17b and 18b show, the proposed strategy successfully reduces the vibration amplitude in the membrane. This demonstrates the effectiveness of the proposed membrane vibration-isolation strategy. Figure 18a shows that the web-cable LQ-substructure controller does not alleviate the web-

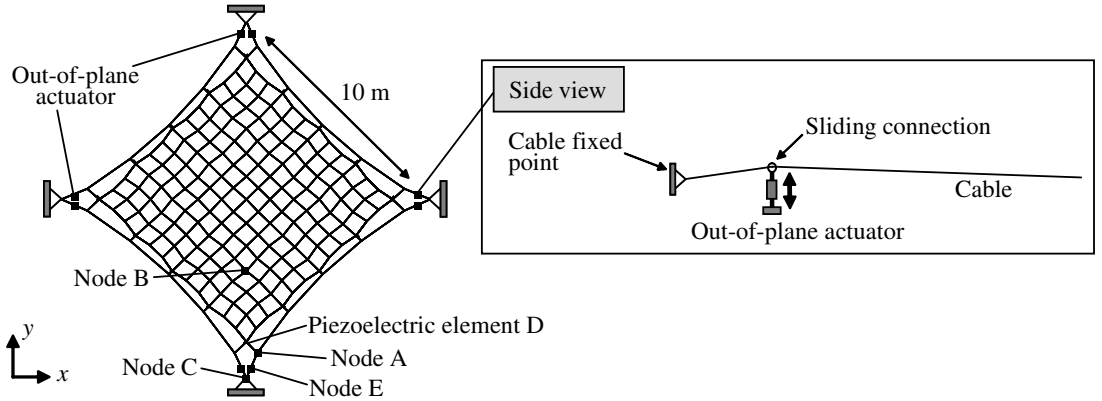

Fig. 10 Finite-element model with LQ-substructure controllers on web cables.

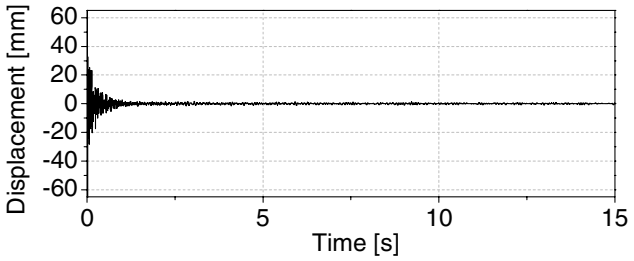

a) On outer perimeter cable (Node A)

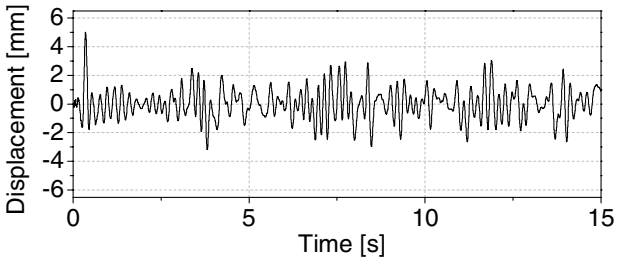

b) On membrane (Node B)

Fig. 11 Response with both LQ-substructure control and cable-tension control: A velocity impulse is applied at node C at $t = 0$.

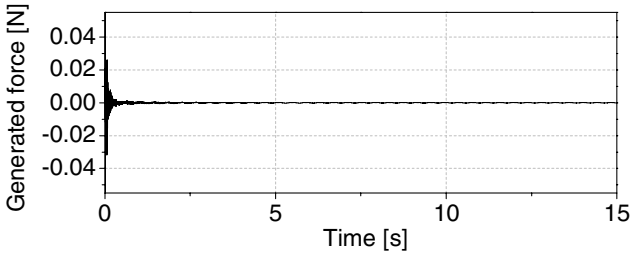

a) Generated force in piezoelectric element D

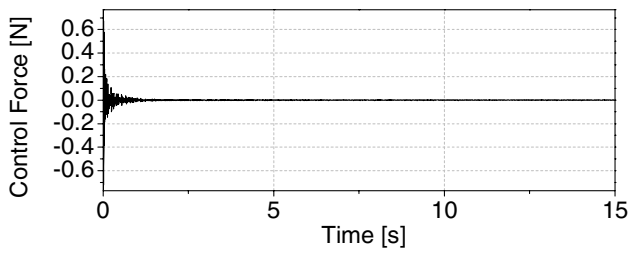

b) Control force applied at Node E

Fig. 12 Generated force by two kinds of controllers.

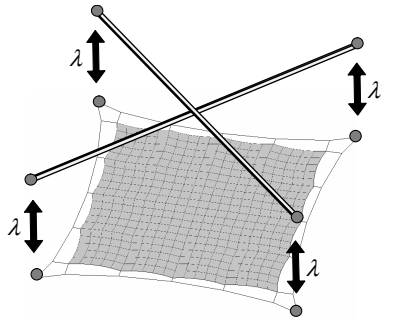

Fig. 13 Extension of proposed vibration-isolation strategy to compressive supports.

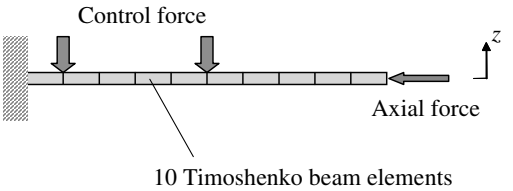

Fig. 14 Finite-element model for beam only vibration control.

cable vibration as effectively as in the preceding model without the beams (Fig. 11a). This is understood as a result of model perturbations in the web-cable substructures. Unlike the preceding analysis, the web-cable substructures are perturbed from both the support corners and the membrane interfaces. These perturbations degrade the performance of the LQ controllers, which are based on the linearly approximated model. In the proposed dual-control strategy, the LQ-substructure controllers may be turned off while they are unstable due to the perturbations. Even so, the system vibration can be dissipated by the cable-tension controllers, which are always stable.

VII. Discussion

The results of the numerical simulations above provide an insight that the dynamic tailoring of the suspension-cable design may

Table 4 Beam properties

Category	Value
Length	8.84 m
Bending stiffness	2660 Nm^2
Linear mass	34.0 g/m
Axial force	17.0 N

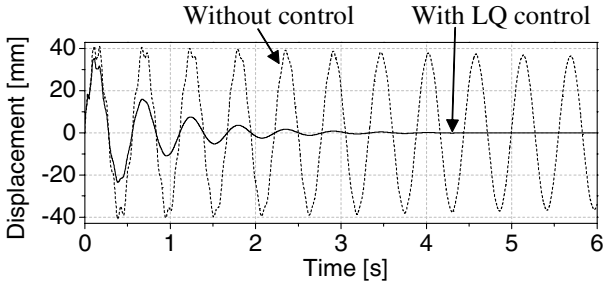

Fig. 15 Uncontrolled and controlled responses at the beam tip with beam LQ controller: A velocity impulse is applied at the tip at $t = 0$.

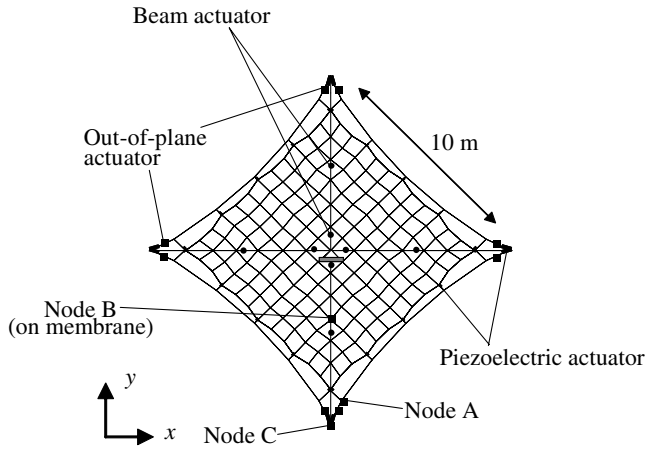

Fig. 16 Finite-element model to demonstrate beam/membrane/cable-coupled control.

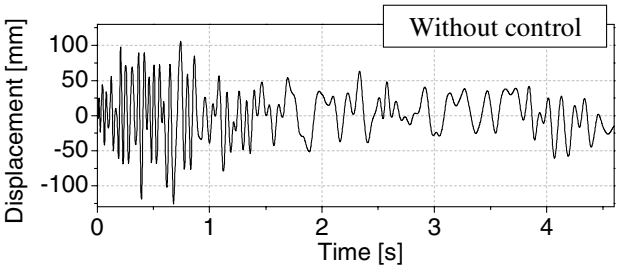

a) On outer perimeter cable (Node A)

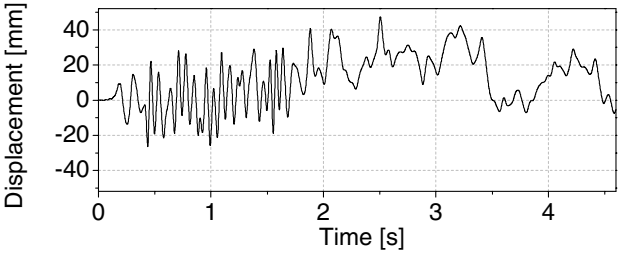

b) On membrane (Node B)

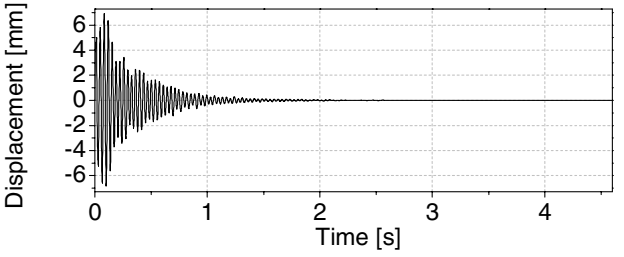

c) On beam tip (Node C)

Fig. 17 Uncontrolled response of beam/membrane/cable-coupled model.

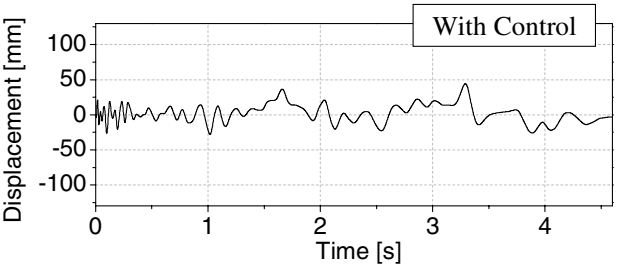

a) On outer perimeter cable (Node A)

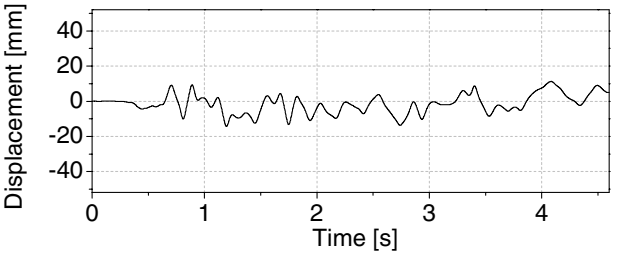

b) On membrane (Node B)

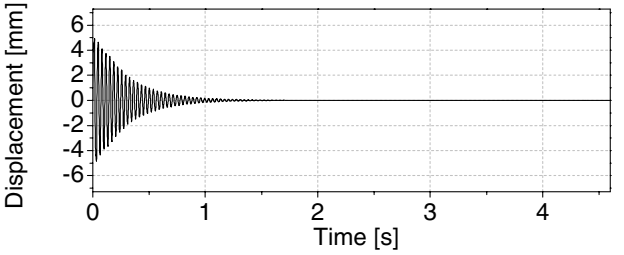

c) On beam tip (Node C)

Fig. 18 Controlled response of beam/membrane/cable-coupled model.

enhance the vibration-isolation effect of the proposed strategy. The simulations show a significant impact of the substructural mode-frequency difference on the controller performance. Table 3 shows the fundamental mode frequencies of each substructure in the analyses. It will be difficult to design the web cables to have as low frequencies as the membrane; thus, the localized-substructure controllers along the web cables cannot effectively absorb the vibration from the membrane, once the membrane starts vibrating. However, it may be possible to tailor the web-cable frequency to be as low as the mode frequencies of the support structures. By this selection, the web cables will efficiently absorb the vibration in the support structures, so that the web-cable substructure controllers can perform more effectively. This will result in more effective vibration isolation for the membrane. The tailoring of the web-cable design will be achieved by changing the connectivity of the cables, changing the cable cross-sectional area, or attaching mass dampers along the cables. This topic is discussed in [43,44].

VIII. Conclusion

The present study has developed a successful vibration-isolation strategy for lightly prestressed membranes in space applications. There are two kinds of controllers: linear theory-based localized controllers for suspension cables and distributed cable-tension controllers at membrane/cable interfaces. Control laws for this dual-control system are derived using a partitioned equation of motion, and numerical simulations using a geometrically nonlinear finite-element method demonstrate the effectiveness of the proposed strategy. The simulation extends the proposed strategy to compressive-support structures and shows the advantages and limitations of the strategy. The localized controllers are better at dealing with small deformations, whereas the distributed ones are better at dealing with large deformations, ensuring stability for the highly nonlinear system. Thus, the two control systems complement

each other, enabling a synergetic performance for effective membrane-vibration isolation.

Acknowledgements

This research is partially supported by the research grant from NASA Langley Research Center, NAG-1-02009. We thank W. Keith Belvin for his encouragement and constructive discussions. H. Sakamoto is supported by the Japan Society for the Promotion of Science (JSPS) Postdoctoral Fellowships for Research Abroad 2005.

References

[1] Lake, M. S., Peterson, L. D., and Levine, M. B., "A Rationale for Defining Structural Requirement for Large Space Telescopes," *Journal of Spacecraft and Rockets*, Vol. 39, No. 5, Sept.–Oct. 2002, pp. 674–681.

[2] Sakamoto, H., Miyazaki, Y., and Park, K. C., "Evaluation of Cable Suspended Membrane Structures for Wrinkle-Free Design," AIAA Paper 2003-1905, 2003.

[3] Sakamoto, H., Park, K. C., and Miyazaki, Y., "Dynamic Wrinkle Reduction Strategies for Cable Suspended Membrane Structures," *Journal of Spacecraft and Rockets*, Vol. 42, No. 5, Sept.–Oct. 2005, pp. 850–858.

[4] Connell, J. W., and Watson, K. A., "Materials for Inflatables in Space," *Gossamer Spacecraft: Membrane and Inflatable Structures Technology for Space Applications*, edited by C. H. Jenkins, Vol. 191, Progress in Astronautics and Aeronautics, AIAA, New York, 2001.

[5] Gaspar, J. L., Mann, T., Behun, V., Wilkie, W. K., and Pappa, R., "Development of Modal Test Techniques for Validation of a Solar Sail Design," AIAA Paper 2004-1665, 2004.

[6] Wilkie, W. K., Inman, D. J., Lloyd, J. M., and High, J. W., "Anisotropic Piezocomposite Actuator Incorporating Machined PMN-PT Single Crystal Fibers," AIAA Paper 2004-1889, 2004.

[7] Pappa, R. S., Giersch, L. R., and Quagliaroli, J. M., "Photogrammetry of a 5m Inflatable Space Antenna with Consumer-Grade Digital Cameras," *Experimental Techniques*, Vol. 25, No. 4, 2001, pp. 21–29; also NASA TM-2000-210627, 2000.

[8] Jenkins, C. H., Gough, A. R., Pappa, R. S., Carroll, J., Blandino, J. R., Miles, J. J., and Rakoczy, J., "Design Considerations for an Integrated Solar Sail Diagnostics System," AIAA Paper 2004-1510, 2004.

[9] Miyazaki, Y., "Wrinkle/Slack Model and Finite Element Dynamics of Membrane," *International Journal for Numerical Methods in Engineering*, Vol. 66, No. 7, May 2006, pp. 1179–1209.

[10] Miyazaki, Y., and Kodama, T., "Formulation and Interpretation of the Equation of Motion on the Basis of the Energy- Momentum Method," *Journal of Multi-Body Dynamics*, Vol. 218, No. 1, March 2004, pp. 1–7.

[11] Miyazaki, Y., and Uchiki, M., "Deployment Dynamics of Inflatable Tube," AIAA Paper 2002-1254, 2002.

[12] Shaker, F. J., "Effect of Axial Load on Mode Shapes and Frequencies of Beams," NASA TN D-8109, Dec. 1975.

[13] Jenkins, C. H., Wilkes, J. M., and Marker, D. K., "Improved Surface Accuracy of Precision Membrane Reflecors through Adaptive Rim Control," AIAA Paper 98-1983, 1998.

[14] Bishop, J. A., "Shape Correction of Initially Flat Membranes by a Genetic Algorithm," AIAA Paper 98-1984, 1998.

[15] Peng, F., Hu, Y. R., and Ng, A., "Active Control of Inflatable Structure Membrane Wrinkles Using Genetic Algorithm and Neural Network," AIAA Paper 2004-1827, 2004.

[16] Salama, M., Kuo, C. P., Garba, J., Wada, B., and Thomas, M., "On-Orbit Shape Correction of Inflatable Structures," AIAA Paper 94-1771, 1994.

[17] Utku, S., Kuo, C. P., Garba, J. A., and Wada, B. K., "Shape Control of Inflatable Reflectors," *Journal of Intelligent Material Systems and Structures*, Vol. 6, July 1995, pp. 550–556.

[18] Scharf, D. P., Hyland, D. C., and Washabaugh, P. D., "Electrostatic Control of a Membrane Using Adaptive Feedback Linearization," AIAA Paper 98-4139, 1998.

[19] Main, J. A., and Martin, J., "Maintenance of Inflated Structure Shape Using Electron Gun Controlled Piezoelectric Materials," AIAA Paper 98-1982, 1998.

[20] Gorinevsky, D., Hyde, T., and Cabuz, C., "Distributed Localized Shape Control of Gossamer Space Structures," AIAA Paper 2001-1197, 2001.

[21] Furuya, H., Miyazaki, Y., and Akutsu, Y., "Experiments on Static Shape Control of One-Dimensional Creased Membrane by Piezoelectric Films," AIAA Paper 2002-1377, 2002.

[22] Rogers, J. W., and Agnes, G. S., "Active Axisymmetric Optical Membranes," AIAA Paper 2002-1450, 2002.

[23] Maji, A., Montemerlo, P., and Ng, T., "Shape Correction of Inflatable Membranes by Rigidization and Actuation," *Journal of Spacecraft and Rockets*, Vol. 41, No. 4, July–Aug. 2004, pp. 558–563.

[24] Natori, M., Miura, K., Ichida, K., and Kuwao, F., "Vibration Control of Membrane Space Structures through the Change of Support Tension," *40th Congress of the International Astronautical Federation*, AIAA, Washington, DC, 1989; also IAF Paper 89-335.

[25] Sodano, H. A., Park, G., and Inman, D. J., "Vibration Testing and Control of an Inflatable Torus Using Multiple Sensors/Actuators," AIAA Paper 2003-1044, 2003.

[26] Solter, M. J., Horta, L. G., and Panetta, A. D., "A Study of a Prototype Actuator Concept for Membrane Boundary Control," AIAA Paper 2003-1736, 2003.

[27] Glaese, R. M., and Bales, G. L., "Demonstration of Dynamic Tailoring for Gossamer Structures," AIAA Paper 2004-1824, 2004.

[28] Park, K. C., and Kim, N., "A Theory of Localized Vibration Control via Partitioned LQR Synthesis," Center for Aerospace Structures, University of Colorado at Boulder, CU-CAS-98-13, Sept. 1998.

[29] Young, K. D., "Distributed Finite-Element Modeling and Control Approach for Large Flexible Structures," *Journal of Guidance, Control, and Dynamics*, Vol. 13, No. 4, July–Aug. 1990, pp. 703–713.

[30] Sunar, M., and Rao, S. S., "Substructure Decomposition Method for the Control Design of Large Flexible Structures," *AIAA Journal*, Vol. 30, No. 10, 1992, pp. 2573–2575.

[31] Su, T., Babuska, V., and Craig, R., "Substructure-Based Controller Design Method for Flexible Structures," *Journal of Guidance, Control, and Dynamics*, Vol. 18, No. 5, Sept.–Oct. 1995, pp. 1053–1061.

[32] Balas, M. J., and Canavin, J. R., "An Active Modal Control System Philosophy for a Class of Large Space Structures," *Proceedings of Dynamics and Control of Large Flexible Spacecraft*, AIAA, Blacksburg, VA, 1977, pp. 271–285.

[33] Morita, Y., and Park, K. C., "Localized Vibration Control: Theory and Demonstration," *Proceedings of the 23rd International Symposium on Space Technology and Science*, Japan Society for Aeronautical and Space Sciences, Tokyo, Japan, 2002 [CD-ROM]; also No. ISTS 2002-d-58.

[34] Ishimura, K., Natori, M. C., and Higuchi, K., "An Autonomous Distributed Control of Free-Floating Variable Geometry Trusses," AIAA Paper 99-1535, 1999.

[35] Ishimura, K., and Natori, M. C., "Deployment Behavior of Modularized Structures," *Adaptive Structures and Material Systems*, Vol. 60, American Society of Mechanical Engineers, New York, 2000, pp. 425–432.

[36] Sakamoto, H., Natori, M. C., and Miyazaki, Y., "Deflection of Multicellular Inflatable Tubes for Redundant Space Structures," *Journal of Spacecraft and Rockets*, Vol. 39, No. 5, Sept.–Oct. 2002, pp. 695–700.

[37] Mikulas, M. M., and Adler, A. L., "Rapid Structural Assessment Approach For Square Solar Sails Including Edge Support Cords," AIAA Paper 2003-1447, 2003.

[38] Locatelli, G., *Piezo-Actuated Adaptive Structures for Vibration Damping and Shape Control—Modeling and Testing*, VDI Verlag, Düsseldorf, Germany, 2001.

[39] Park, K. C., Felippa, C. A., and Gumaste, U. A., "A Localized Version of the Method of Lagrange Multipliers and its Applications," *Computational Mechanics*, Vol. 24, No. 6, Jan. 2000, pp. 476-490.

[40] Park, K. C., and Felippa, C. A., "A Variation Principle for the Formulation of Partitioned Structural Systems," *International Journal for Numerical Methods in Engineering*, Vol. 47, Jan. 2000, pp. 395–418.

[41] Belvin, W. K., and Park, K. C., "Structural Tailoring and Feedback Control Synthesis: An Interdisciplinary Approach," *Journal of Guidance, Control, and Dynamics*, Vol. 13, No. 3, May–June 1990, pp. 424–429.

[42] Bellman, R., *Introduction to Matrix Analysis*, 2nd ed., McGraw–Hill, New York, 1970.

[43] Sakamoto, H., and Park, K. C., "Advanced Cable Boundary Design in Membrane Structures in Membrane Space Structures," AIAA Paper 2005-1973, 2005.

[44] Sakamoto, H., and Park, K. C., "Localized Vibration Isolation Strategy for Low-Frequency Excitations in Membrane Space Structures," *Journal of Vibration and Acoustics* (to be published).

G. Agnes
Associate Editor